Implementation of a Grey Prediction System Based on Fuzzy Inference for Transmission Power Control in IoT Edge Sensor Nodes

Guillermo Moreno, Gabriel Mujica, *Member, IEEE*, Jorge Portilla, *Senior Member, IEEE*, and Jin-Shyan Lee, *Senior Member, IEEE*

***Abstract*—The rapid growth of the Internet of Things (IoT) has expanded the research and implementation of wireless sensor networks (WSNs) in various application domains. However, the challenges associated with resource-constrained sensor nodes and the need for ultralow power consumption pose significant problems. One fundamental strategy to address these challenges is transmission power control (TPC), which adjusts the transmission power of nodes to optimize network performance and lifetime. While traditional methods have focused on static scenarios, this work presents a novel approach for mobile WSNs based on a grey-fuzzy-logic TPC (Grey-FTPC). The proposed system integrates grey prediction techniques with fuzzy inference to dynamically adapt transmission power levels. Unlike previous simulations, this work focuses on real implementations, considering practical aspects of WSN deployments and the characteristics of embedded sensor platforms. The objectives of this work are twofold: 1) to implement a Grey-FTPC on an IoT embedded hardware platform, ensuring compatibility with IEEE 802.15.4 networks and 2) to propose a runtime adaptive link recovery mechanism to enhance the robustness of the adaptive TPC in mobile and unstable contexts. Additionally, a multihop mobile Grey-FTPC strategy is introduced, enabling collaborative transmission power adaptation among sensor nodes. Experimental tests demonstrate the high-prediction accuracy of the proposal even in multihop scenarios, confirming the system's scalability. Results also show that the proposed system outperforms other strategies in terms or energy consumption, achieving up to 43% of gains depending on the scenario.**

***Index Terms*—Extreme edge computing, grey prediction, Internet of Things (IoT), mobile wireless sensor networks (WSNs).**

I. Introduction

OVER the past few years, the rise of the Internet of Things (IoT) paradigm has significantly expanded the scope of research and implementation of wireless sensor networks (WSNs) technologies. This expansion encompasses a diverse range of application domains, such as Smart Cities, Industry 4.0 and 5.0, intelligent transportation systems, e-healthcare, and smart agriculture, among others [1], [2], [3], [4], [5]. Unlike traditional WSN infrastructures, the IoT architecture incorporates a sophisticated array of technological and abstraction layers that enable seamless integration between on-site sensor nodes and cloud services. This integration has stimulated the emergence of new research fields in edge-cloud orchestration [6], cloud, fog, and edge computing [7], heterogeneous system integration [8], and dense network management [9].

Nevertheless, the problems associated with the WSNs are still in ongoing research lines, and they are gaining importance as the number of tiny devices in the era of IoT is expected to grow exponentially [10]. These problems are extrapolated to what is known as the extreme edge of the IoT [11], which is the bottom layer where the sensor devices are located. The main issues that must be tackled are related to the resource-constrained nature of these nodes, their limited bandwidth and processing capabilities, all of it in relation with the need of ultralow power consumption of the nodes to ultimately extend the lifetime of the network. Since the extreme edge of the IoT must be autonomous, self-managed capabilities, reconfiguration and reprogramming strategies, along with runtime node/network adaptation to dynamic conditions are key aspects to the success of the system in the target environment [12].

Apart from the consideration of ultralow power hardware technologies in the context of processing, wireless communication, routing capabilities, and energy harvesting [13] one of the fundamental strategies to reduce the power consumption in WSNs and IoT edge sensor networks is the concept of transmission power control (TPC) [14], which deals with the adaptation of the transmission power of the nodes based on considering a tradeoff between the quality of the links in the network, data rate, quality of the service, path selection and ultimately the lifetime of the overall network. The TPC has been addressed from different angles during the last years, although most of the solutions have been proposed from a simulation perspective, not completely covering practical aspects of real WSN deployments and the challenges associated with the behavior and technical characteristics of embedded sensor platforms.

Moreover, while most traditional methods tackle the problem of TPC from a static point of view, that is, considering

Manuscript received 22 December 2023; revised 6 February 2024; accepted 22 February 2024. Date of publication 5 March 2024; date of current version 23 May 2024. This work was supported by the Project PID2020-116417RB-C41 (TALENT-HIPSTER) funded by MCIN/AEI/10.13039/501100011033. *(Corresponding author: Gabriel Mujica.)*

Guillermo Moreno, Gabriel Mujica, and Jorge Portilla are with the Centro de Electrónica Industrial, Universidad Politécnica de Madrid, 28006 Madrid, Spain (e-mail: guillermo.morvazquez@alumnos.upm.es; gabriel.mujica@upm.es; jorge.portilla@upm.es).

Jin-Shyan Lee is with the Department of Electrical Engineering, National Taipei University of Technology, Taipei 10608, Taiwan (e-mail: jslee@mail.ntut.edu.tw).

Digital Object Identifier 10.1109/JIOT.2024.3373263

that the sensor nodes hardly have mobility once they are deployed in the target environment, the work presented in [15] proposes a novel approach for predicting the next transmission power level based on a grey-fuzzy-logic TPC (Grey-FTPC) for mobile WSNs, by integrating a grey prediction technique with a fuzzy inference system to cope with the dynamics of these sensor network scenarios. However, although that work provided the baseline to apply a lightweight prediction system without the need of a high set of past measurements to carry out the predictions, the theoretical model lacks real hardware and software considerations for their proper implementation in a WSN sensor platform. This work addresses these issues by optimizing the work proposed in [15] with an improved Grey-FTPC and its implementation in a modular IoT hardware platform.

Regarding the analysis of state-of-the-art solutions for TPC, while in [15] the most widespread and traditional proposals were already discussed, newer works focus on the use of artificial intelligence techniques for sensor node transmission adaptation, or the application of TPC in various research fields as an enabler to optimize the lifetime of the target network, such as in the case of wearable devices and body area sensor networks. Recent works apply machine learning to enable TPC, such as the so called cognitive TPC. Pace et al. [16] applied the idea of in-node reinforcement learning agents to minimize the energy level. The problem is approached from a node-pairing perspective, ignoring the dynamics of multihop communication topologies in the solution. Moreover, the dynamics associated with node mobility are not contemplated. Wang et al. [17] addressed a joint optimization of transmission power selection together with time slot allocation in the context of body area networks, by applying a deep reinforcement learning strategy. The work considers predefined path loss values for the simulation setup and no additional details related to real IoT sensor platforms are included to test the solution in an actual implementation, while some assumptions do not fit properly with real WSN behavior, such as number of bits per frame and path loss range, among others.

Sodhro et al. [18] proposed a solution for TPC in the context of healthcare, particularly related to body sensor networks, where the variation of the received signal strength indicator (RSSI) parameter based on body postures is studied. While the duty-cycle variation for adapting the task execution period is taken into account, the approach only considers a single-start topology, leaving out multihop communication and diversity in topology adaptation. Moreover, results are validated only through simulations. Other works also focus on the application of TPC in body sensor networks, such as in [19], where a different approach from controlling the transmission power is presented. Authors highlighted the idea of analyzing how specific positions of the sensor nodes in body may affect the transmission performance, whether there is movement or not. By relating the movement of the body with the transmission power, the system tries to minimize the packet exchange between the sensor nodes and the sink. Obliviously, this type of solution is very specific to body area sensor network applications.

Chen et al. [20] expanded the study of the TPC by analyzing the impact of packet size and transmission delay for the power management of the WSN. They assume centralized time-division multiple access (TDMA)-based strategy for the network, as well as synchronization of the nodes. The work is studied from a simulation perspective, and theoretical characteristics from the MICA2 [21] sensor nodes are used. Moreover, authors do not consider mobility of the networks, and the implications of such dynamics in unstable environments and thus how the next transmission power can be predicted based on the network current and previous conditions.

The concept of TPC is also applied in other types of wireless technologies for WSNs and IoT, such as LoRa [22], where a tradeoff between distance coverage and power consumption is crucial. Susan Philip and Singh [23] proposed a dynamic TPC algorithm for LoRa-based air quality monitoring system, to minimize the power consumption of the sensor nodes and thus extend their lifetime. This type of LoRa-based networks is static while the main challenge is to rise long-range distances from the node to the gateway. Moreover, they are conceived as star networks, so the problem of multihop communication is not tackled.

Other works try to apply TPC in Internet of Underwater Things (IoUT), where transmission quality versus lifetime is key for the network and data integrity. Coutinho et al. [24] proposed the combination of opportunistic routing with TPC based on neighbor information to cooperatively select the closest node to transmit the packet to the sink, so that the data rate can be improved while the power consumption can be kept in such conditions. Similarly, in [25] the concept of transmission power adaptation in underwater sensor networks is studied, aiming to optimize cluster head selections with reduced interference and increased network lifetime. Additionally, authors propose the use of mobile sinks to evaluate how distance threshold definitions can improve the data transmission collaboration among the participant sensors with respect to the cluster heads.

As mentioned before, this work focuses on addressing a real implementation of a mobile Grey-FTPC from the basis of the proposal in [15] but considering its integration with an IoT embedded hardware platform, that is, a real implementation in sensor nodes. Unlike most works that address the problem of transmission power decision in static scenarios and mainly from a simulation perspective, in this work, which is the result of a collaboration between international institutions, and an extension of the work carried out in [15], a lightweight grey prediction strategy combined with fuzzy inference is developed for a multihop WSN, thus covering the limitations of the previous work. In this sense, the main objectives and contributions of this work are summarized as follows.

1) A real implementation of a grey-prediction Fuzzy Inference-based Adaptive TPC for mobile WSNs, considering the practical implications of IEEE 802.15.4-based networks and technological aspects for its proper integration into a real IoT sensor node platform. The system is divided into a sink implementation and in-node embedded implementation, and cooperation among the sensor nodes is carried out to properly perform the transmission power configuration dynamically. The implementation is presented in detail together with

graphical functional diagrams throughout the article to support the description and its usability.

2) A runtime adaptive link recovery (ALR) for finite maximum coverage is proposed and implemented in the embedded solution, which allows increasing the reliability and robustness of the ATPC in mobile and unstable contexts. While simulation approaches consider a wide range of coverage or bidirectional links, in real scenarios the sensor network must deal with asymmetric conditions that may significantly degrade the result of the transmission power configuration.
3) A multihop mobile Grey-FTPC strategy is proposed, which relies on the collaboration between the wireless sensor nodes to perform the transmission power adaptation in a seamless fashion from the point of view of the sink node, that is, while the Grey-FTPC remains transparent in relation with the network topology, the multihop TPC technique gives support to carry out the dynamic adaption in inner transmission paths. Results show that the prediction levels are high even when the number of hops increases, so the scalability of the system is evaluated and verified.

Several experimental tests have been carried out to deeply compare the outcome of the prediction engine with respect to the real behavior of the WSN, and results allowed refining and optimizing the mobile Grey-FTPC implementation to better fit the system application to unstable environments.

The remainder of this article is summarized as follows. In Section II the Grey Prediction model theory is introduced to provide a quick overview of the applied predictive model with a reduced amount of data set. Then, in Section III the implementation details of the grey fuzzy-inference-based prediction system for TPC are deeply addressed, describing the different functional components both at base station (BS) side and in-node embedded side that compose the complete system, considering a real extreme edge IoT modular sensor platform. Section IV is devoted to present the main optimizations introduced in the proposed system, considering the real characteristics and behavior of WSN in actual hardware and application contexts, while in Section V the experimental results and the analysis of the system verification in a real deployment are addressed, together with an energy consumption analysis of the proposed solution in comparison with other strategies. Finally, conclusions and future lines of work are presented in Section VI.

II. Theory of the Grey Prediction Model

As presented in the previous work [15] and briefly summarized in this section, the grey model preserves prediction accuracy even with a small data set. For each sensor node, a predictive grey model of first-order and one-variable, the RSSI data received, is implemented. The model is built from the last n RSSI data received, being sufficient with the last four values

$$x^{(0)} = \left(x^{(0)}(1), x^{(0)}(2), \ldots, x^{(0)}(n)\right), \quad n \geq 4. \tag{1}$$

The accumulated sequence of the input data increases the accuracy of the prediction and is obtained from (1) as

$$x^{(1)}(k) = \sum_{i=1}^{k} x^{(0)}(i), \quad k = 2,\ 3, \ldots,\ n \tag{2}$$

$$\begin{aligned} x^{(1)} &= \left(x^{(1)}(1), x^{(1)}(2), \ldots, x^{(1)}(n)\right) \\ &= x^{(0)}(1), \sum_{i=1}^{2} x^{(0)}(i), \ldots, \sum_{i=1}^{n} x^{(0)}(i). \end{aligned} \tag{3}$$

The grey differential equation for a $GM(1, 1)$ corresponds to (5). The $z^{(1)}$ could be obtained according to Table II from the average of the $x^{(1)}$ data

$$\frac{\partial x^{(1)}(k)}{\partial k} + az^{(1)} = b \tag{4}$$

$$\begin{aligned} z^{(1)}(k) &= \frac{1}{2} \times \left(x^{(1)}(k) + x^{(1)}(k-1)\right) \\ k &= 2,\ 3, \ldots, n. \end{aligned} \tag{5}$$

The coefficients of a and b are estimated by solving (5) with the least-squares method

$$\left[\hat{a}\ \hat{b}\right]^T = \left(A^T A\right)^{-1} A^T X \tag{6}$$

$$A = \begin{bmatrix} -z^{(1)}(2) & 1 \\ -z^{(1)}(3) & 1 \\ \vdots & \vdots \\ -z^{(1)}(n) & 1 \end{bmatrix} \tag{7}$$

$$A = \begin{bmatrix} x^{(0)}(2) \\ x^{(0)}(3) \\ \vdots \\ x^{(0)}(n) \end{bmatrix}. \tag{8}$$

With the initial condition (10), the solution of the differential equation is as

$$\hat{x}^{(1)}(k) = \left(x^{(0)}(1) - \frac{\hat{b}}{\hat{a}}\right) e^{-\hat{a}(k-1)} + \frac{\hat{b}}{\hat{a}}$$

$$k = 2,\ 3, \ldots,\ n \tag{9}$$

$$\hat{x}^{(1)}(1) = x^{(1)}(1) = x^{(0)}(1). \tag{10}$$

The result of $\hat{x}^{(0)}(k)$ in (11) refers to the k RSSI data received. Defining $k > n$ results in a future prediction of the RSSI

$$\begin{aligned} \hat{x}^{(0)}(k) &= \hat{x}^{(1)}(k) - \hat{x}^{(1)}(k-1) \\ &= \left(1 - e^{\hat{a}}\right)\left(x^{(0)}(1) - \frac{\hat{b}}{\hat{a}}\right) e^{-\hat{a}(k-1)} \\ k &= 2,\ 3, \ldots,\ n. \end{aligned} \tag{11}$$

To benefit from the small set of data in the GM, the algorithm has been designed for the values $n = 4$ and $k = 6$.

III. Grey-FTPC Implementation

The implementation is based on the mode of operation described in [15], i.e., at system initialization, the transmission power of each node is set up to the minimum necessary

Fig. 1. CC2520-based cookie hardware layer used for the Grey-FTPC implementation.

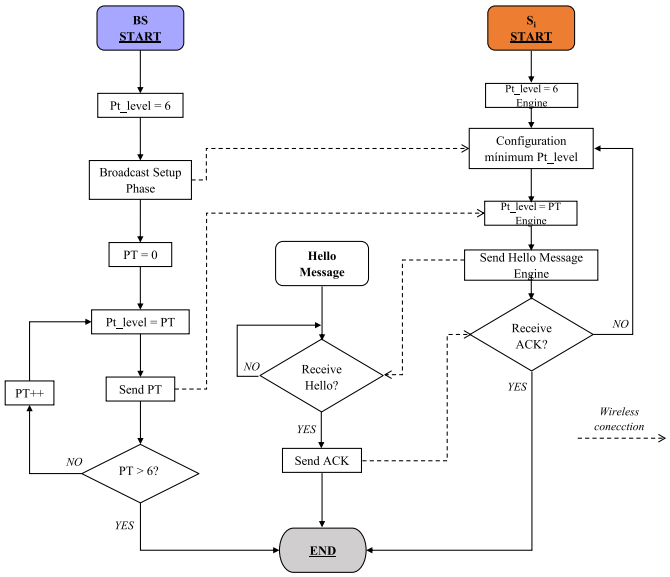

Fig. 2. Setup phase diagram between the BS and the sensor nodes, indicating the wireless communication data exchange among them during the process.

(setup phase). Then, the power is periodically adjusted using the Grey-FTPC algorithm (adjustment phase). Packet transmission and power level configuration during these phases are implemented directly on the sensor nodes. The WSN is initially deployed in a star configuration, with a stationary BS and the rest of the mobile sensor nodes connected to it with bidirectional and wireless communication. The Grey-FTPC algorithm is implemented on a PC connected to the BS through a serial interface (UART). The hardware used for the sensor nodes is a modular WSN platform for IoT called Cookies [26], [27], which is a flexible and adaptable architecture that allows fast integration of IoT technologies in the form of four modular layers, i.e., processing, communication, power and sensing. Depending on the target application, the sensor node can be set up with the most suitable layers according to the requirements to be met. In this case, a configuration based on a CC2520 [28] transceiver in the communication layer, and a ADuC841 MCU [29] in the processing layer is used to carry out the real implementation of the Grey-FTPC. Fig. 1 shows the CC2520-based Cookie hardware layer implemented for IEEE 802.15.4 wireless communication, which includes the vertical connectors that are compliant with the modular interface of the Cookie architecture.

Unlike the previous work, here the real sensor nodes are within the closed loop of operation, providing real dynamic behavior and actual parameters to the optimization engine. Moreover, while the previous work assumed a centralized TDMA-based communication, in this work the IEEE 802.15.4 standard is used as the baseline physical and MAC layers for the wireless communication, which is the most widespread standard for resource-constrained sensor nodes in IoT. Therefore, a carrier sense multiple access with collision avoidance (CSMA/CA) medium access control mechanism is used.

A. Setup Phase

Once the sensor nodes are deployed in the network, they are reset to initialize their operation. With the reset, the node configures the maximum transmission power and starts sending packets to the BS periodically. The packets contain the node ID and power level at the time the packet is sent, Pt_level_k.

After all sensor nodes have been reset, the BS is also reset starting the *SetupPhase*. The BS is initially configured with maximum transmission power and broadcasts to all nodes it can reach, announcing the start of the *SetupPhase*. If a node receives this broadcast, it waits for the next message from the BS, which determines the minimum power to be configured. The BS configures the transmission power at all possible levels, from minimum to maximum, indicating this level in a new broadcast. When the sensor node receives one of these messages, it sets its power to the proposed level. To ensure this is the minimum transmission power that ensures communication, a *HelloMessage* is sent back to the BS. If the sensor node receives an Acknowledgment *ACK* in response to the *HelloMessage*, it keeps the set power and ends the *SetupPhase*. However, if it receives a *NOACK*, then it waits for the next message sent by the BS which will contain a higher power level, sending a new *HelloMessage* with this transmission power. After the BS has set the maximum power level and has sent the broadcast with this level to the nodes, the *SetupPhase* ends, and the *AdjustmentPhase* starts. Fig. 2 shows the *SetupPhase* diagram.

B. Adjustment Phase

The BS receives the packets sent periodically by the sensor nodes. The RSSI in the transmission of the packet, $RSSI_k$, is calculated in the BS and added to the content of the packet. Then, the BS sends the packet data (ID, $RSSI_k$, and Pt_level_k to the input of the Grey-FTPC algorithm implemented in the PC. The $RSSI_k$ is introduced in the GM of the corresponding sensor node identified by its ID. The GM provides new data, $RSSI_{k+1}$, which is a future prediction of the signal strength. $RSSI_k$, $RSSI_{k+1}$, and Pt_level_k enter to a fuzzy controller which will decide the adjustment required for the transmission

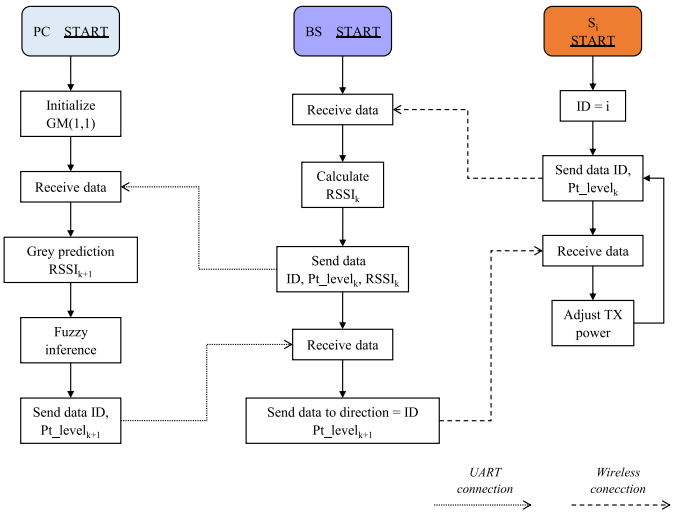

Fig. 3. Adjustment diagram between the Grey-FTPC optimization engine, the BS, and the sensor nodes, indicating the different communication data exchange among them during the process.

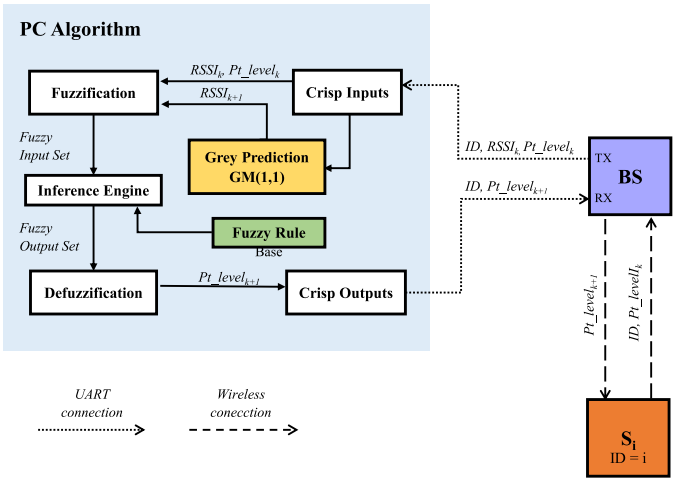

Fig. 4. Packet flow through the dynamic transmission power optimization, where the Grey-FTPC engine, the fuzzy controller, and the embedded sensor node components take part during the process.

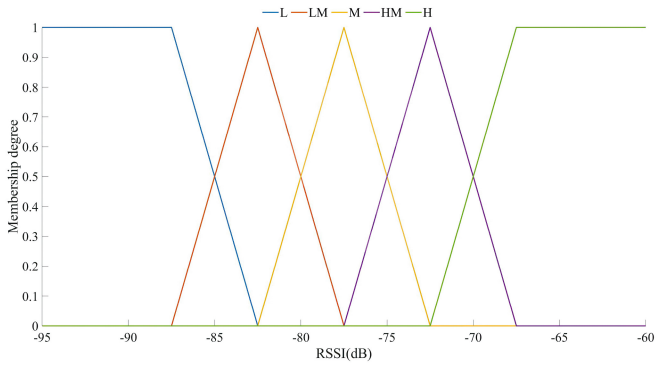

Fig. 5. Fuzzification of the real RSSI range for the WSN.

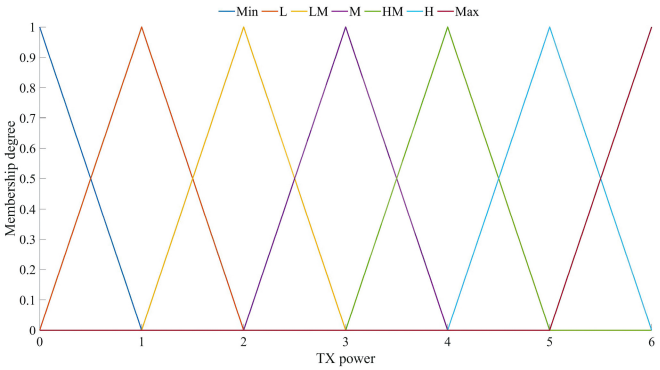

Fig. 6. Fuzzification of the seven transmission power levels of the transceiver (CC2520).

TABLE I
RSSI FUZZY LEVEL INTERVALS ACCORDING TO THE EXPERIMENTAL RANGES

RSSI fuzzy	RSSI crisp
L	[-inf, -85]
LM	[-85, -80]
M	[-80, -75]
HM	[-75, -70]
H	[-70, inf]

power of the sensor node. In case the power needs to be configured, the algorithm generates another packet containing the node ID and the new power level, Pt_level_{k+1}, and sends it to the BS. Finally, the BS distributes these packets to the corresponding sensor nodes to update their transmission power. Fig. 3 shows the *AdjustmentPhase* diagram while in Fig. 4 the packet flow through the different optimization components of this phase is represented.

C. Fuzzy Controller

The fuzzy controller has been implemented in three stages according to [15]. For the fuzzification of the input variables of RSSI and transmission power levels, the triangular membership functions of Figs. 5 and 6 are, respectively, used. The linguistic variables for the five RSSI fuzzy levels are low, low-medium, medium, high-medium, and high (abbreviated as L, LM, M, HM, and H, respectively). The seven fuzzy levels for transmission power level require two additional linguistic variables and these are minimum, low, low-medium, medium, high-medium, high, maximum (abbreviated as Min, L, LM, M, HM, H, and Max, respectively).

The RSSI membership function has been designed based on experimental data obtained from the Grey-FTPC performance in the real WSN. Using the Cookies as the sensor nodes, the RSSI remains in the range of $[-50, -90]$ dBm. The fuzzy levels are equally distributed within this range. In addition, the size of the fuzzy levels is adjusted to maintain the communication of the nodes with the BS with minimum energy consumption.

The conversion of the numerical values of the RSSI to a fuzzy level has been implemented using intervals from the cut-off points of the membership functions. The intervals of the RSSI fuzzy levels are listed in Table I.

The fuzzy levels for transmission power correspond directly to the seven configurable levels of the CC2520 as shown in Table II.

In [15] fuzzy if-then inference rules are predefined, to obtain the new power level Pt_level_{k+1}, which are based on the three

TABLE II
FUZZY LEVELS OF THE TRANSMISSION POWER ACCORDING TO THE AVAILABLE CONFIGURATION IN THE CC2520 TRANSCEIVER

Pt_level fuzzy	Pt_level crisp	TX Power register (hex)
Min	0	03
L	1	2C
LM	2	88
M	3	81
HM	4	32
H	5	AB
Max	6	F2

TABLE III
OPTIMIZATION OF THE NUMBER OF FUZZY INFERENCE RULES FOR THE TRANSMISSION POWER CONFIGURATION

Rule	$RSSI_k$	$RSSI_{k+1}$	inc
1	L	L	1
2	L	LM	1
3	L	M	0
4	L	HM	-1
5	L	H	-2
6	LM	L	2
7	LM	LM	1
8	LM	M	1
9	LM	HM	0
10	LM	H	-1
11	M	L	2
12	M	LM	1
13	M	M	0
14	M	HM	-1
15	M	H	-2
16	HM	L	1
17	HM	LM	0
18	HM	M	-1
19	HM	HM	-1
20	HM	H	-2
21	H	L	2
22	H	LM	1
23	H	M	0
24	H	HM	-1
25	H	H	-1

fuzzy input values. To reduce the number of fuzzy rules, in this work they have been implemented only for RSSI_k and RSSI_{k+1}. As Pt_level_k is not considered in the definition of the rules, Pt_level_{k+1} cannot be obtained. Therefore, the output will be the required power level increase. Table III shows the 25 fuzzy rules established. The new transmission power is given as

$$Pt\_level_{k+1} = Pt\_level_k + inc. \tag{12}$$

In the defuzzification stage, the fuzzy level of Pt_level_{k+1} is converted to the corresponding power level. The new packet generated by the algorithm contains this power level and the corresponding sensor node ID.

IV. GREY-FTPC SYSTEM OPTIMIZATION

A. Runtime Automatic and Adaptive Link Recovery

If the signal between a sensor node and the BS is weak, the GM identifies a low-RSSI value and consequently increases the power. However, the sensor node may lose the signal with the BS before the GM reacts when the RSSI changes abruptly, therefore the new TX power configuration will not be received. This is a condition not contemplated in the previous work and certainly common in real unstable networks.

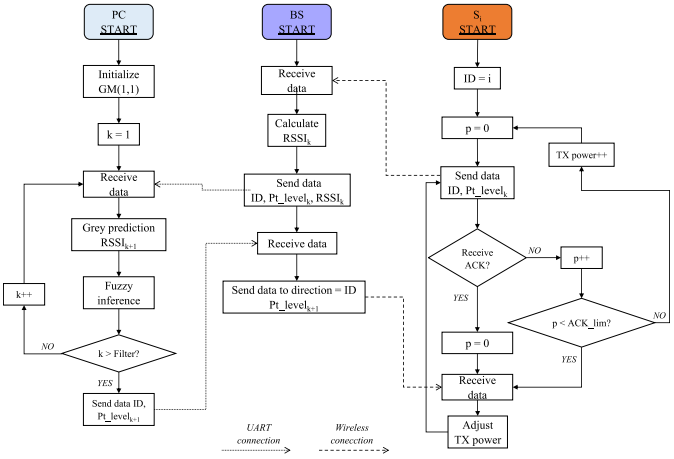

Fig. 7. Updated adjustment phase diagram with the ALR and RSSI filtering for the initial model prediction outcomes.

In this work an embedded automatic power adjustment is implemented at each sensor node to quickly recover the connection to the BS, thus providing an ALR condition. Packets sent periodically by the sensor node receive an *ACK* when they have arrived correctly at their destination and a *NOACK* when they have not. The node is considered to have lost the signal when it receives a certain number of consecutive *NOACKs*. The sensor node increases the transmission power one level after receiving a certain number of consecutive *NOACK*, called *ACK_Lim*. If the newly configured power is not sufficient to reconnect the sensor node and *NOACKs* are received again up to *ACK_Lim*, then another level is incremented. This process is repeated until the sensor node recovers the communication with the BS or until the maximum transmission power level is reached. A small value chosen for *ACK_Lim* allows reducing the time the sensor node remains disconnected but may cause an unnecessary increase of the power in case of losing the signal just for an instant. Therefore, this parameter can be adjusted based on the target application.

B. Filter for the First Model Predictions

The GM is generated from the first n RSSI data received from a sensor node. For the GM to predict the RSSI from the first packet received, it is initialized with n arbitrarily chosen values of RSSI_k, with $k = 1, 2, 3, 4$. These input RSSI values are not expected to correspond to the actual situation of the sensor node. Therefore, the GM predictions using these values will not be accurate and will consequently request an inappropriate change of the transmission power. To avoid this, a filter is implemented in the algorithm to not send the Pt_level_{k+1} obtained from these predictions. Fig. 7 shows the Adjustment Phase diagram updated with the improvements of automatic sensor signal recovery and the filter of the first model predictions.

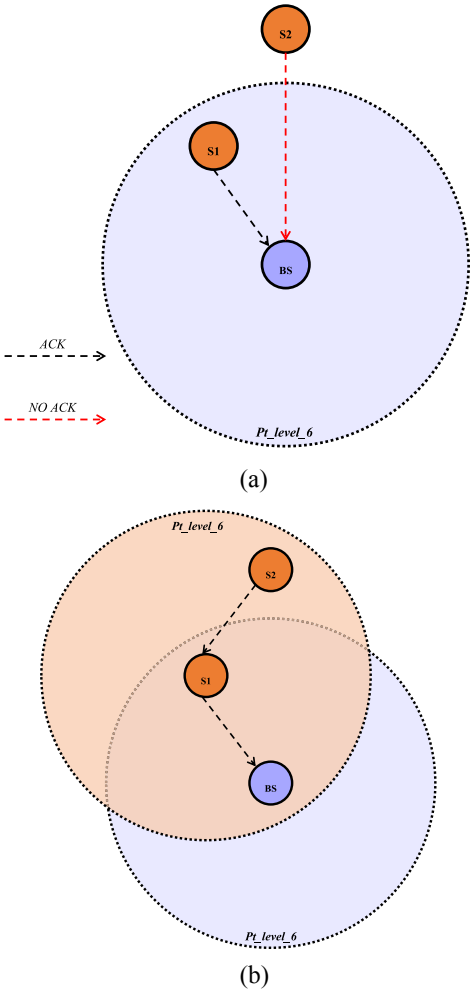

Fig. 8. No direct connection between one of the sensor nodes and the BS, and multihop network support for the transmission power optimization. (a) No direct link between *S2* and the BS. (b) *S1* serves as parent node of *S1* to transparently provide RSSI data to the Grey-FTPC engine through the BS.

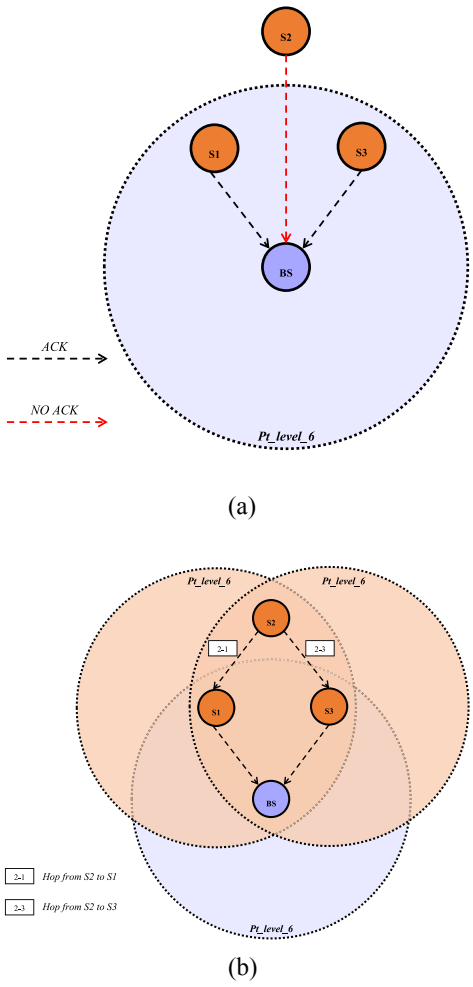

Fig. 9. Multihop parent selection based on dynamic transmission path alternatives, as a result of the mobility of the sensor nodes. (a) Additional nodes taking part of the network and the possible alternatives to select the parent node. (b) Several possible multi-hop transmission paths according to the coverage ranges among the participant nodes in the mobile sensor scenario.

C. Multihop Grey-FTPC

1) Proposal: The implementation of the Grey-FTPC has been initially carried out following the simulation characteristics of [15], using a WSN with a star configuration where each sensor node is directly connected to the BS. This type of network architecture limits the use of the sensor nodes within the range reached by the maximum BS power. The purpose of multihop Grey-FTPC is to extend the operating range of the solution through the consideration of more complex network topologies, by including connections between sensor nodes with the notions of hops. By linking multiple hops between sensor nodes, further points beyond the coverage of the BS are reachable.

To improve the understanding of the multihop contribution, three different cases are given, which can be generalized to the main general coverage situations in mobile wireless sensor deployments. The network map for the first case with the BS and two sensor nodes, S1 and S2, is shown in Fig. 8. S1 is located at a point within the range of BS and S2 outside this range. Hence, there is no direct connection between S2 and the BS, so the multihop configuration is initialized to find an alternative path for the packets sent from S2 to reach the BS. First, it evaluates whether S2 is within the range of any other sensor node in the network. In this case, it is only possible that it is within the range of S1. Thus, the hop is established from S2, as a child sensor, to S1, as a parent sensor, which will be responsible for transmitting the packets from both sensor nodes to the BS.

The packet with the information from S2 includes the RSSI for the hop to S1, so the algorithm optimizes the transmission power of S2 for this new connection. The algorithm is completely transparent to the network architecture, since it receives a packet with the *ID*, RSSI_k, Pt_level_k, and obtains Pt_level_{k+1} for these inputs. The transmission power determined by the algorithm is sent from the BS to the corresponding sensor node in a command packet using the same path. Therefore, although the algorithm does not need to know the network configuration for its operation, each sensor node needs to know its connections to other nodes to send these command packets to their destination.

In the second case in Fig. 9, a similar network is shown but with an additional sensor node, S3, also directly connected to the BS. If S2 is included in the range of S3, there is

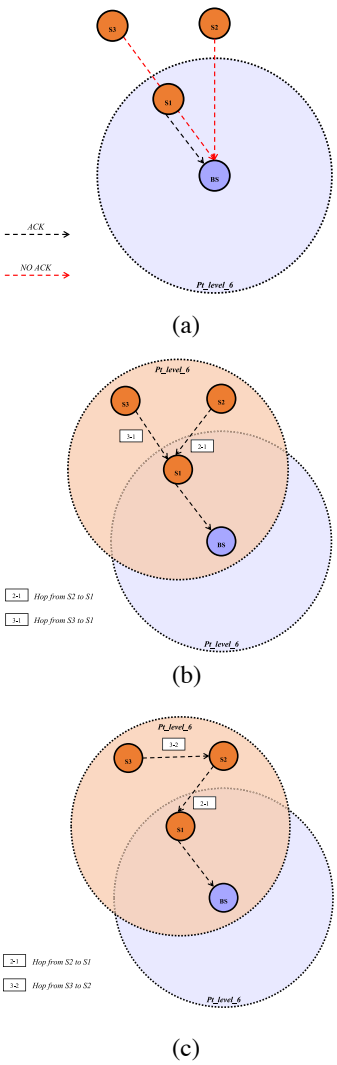

Fig. 10. Alternatives of transmission path reconfiguration according to the update of the sensor node coverage and the RSSI parameter. (a) Nodes move from the original position causing a redistribution of the coverage from the BS and among them, so the multihop transmission paths will be updated. (b) Nodes *S2* and *S3* select S1 as their parent node. (c) Node *S3* select *S2* as parent node once it already set a transmission path to the BS.

another possible path for packets from S2 to reach the BS through the hop from S2 to S3. Depending on whether the hop is to S1 or S3, two paths are available. The criteria established for the decision on the best path are based on the distinction of the RSSI received from the different parent sensor candidates. S2 will choose as the parent sensor the node from which it receives the best RSSI between S1 and S3.

The last case in Fig. 10 shows the scenario where S3 and S2 are both outside the range of BS and have to find an alternative path for transmission, but they are both also within the range of S1. Consider S2 as the first sensor node to perform the multihop configuration. This sensor node has the option to hop to S1 or S3. However, since S3 also has no connection to the BS, the only possible option is a hop to S1. The multihop configuration of the sensor node S3 starts after the configuration of S2 is finished. This sensor node has the option to hop to S1 or S2. In this case, both paths are valid since they

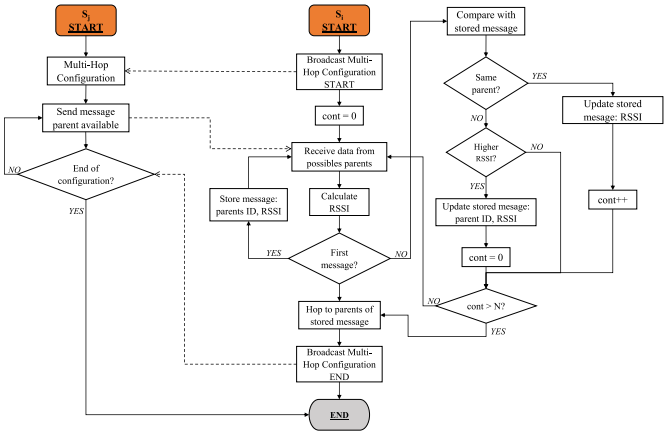

Fig. 11. Hop configuration and parent selection for the multihop Grey-FTPC.

allow the connection to the BS. The parent sensor is chosen by distinguishing again between the RSSI received by each of the candidates, thus the quality of the links is prioritized. If the hop to S1 is chosen, the network is split from S1 into two branches, whereas if the hop to S3 is chosen, a single branch with two hops is obtained.

2) Implementation of the Hop Configuration: When a sensor node loses communication with the BS, automatic adjustment of transmission power is applied according to the number of *NOACKs* received. The power is increased level by level until the connection is recovered. If the maximum power of the sensor node is reached and the connection with the BS has not been recovered, the multihop configuration is started, and a new transmission path is searched for sending messages.

Fig. 11 shows the diagram for the multihop Grey-FTPC configuration. Initially, the sensor node that has lost connection with the BS broadcasts packets requesting candidates as parent node. Nodes receiving these packets respond by sending packets back offering themselves as candidates. The sensor node with no connection to the BS stores the ID and RSSI of the first packet received. The next packet received, if it comes from the same sensor node as the stored packet, the RSSI is updated with the value of the new transmission, and a counter is incremented. However, if the packet comes from a different sensor node, the RSSI is compared between the values obtained by each node. If the RSSI is higher in the sensor node of the first packet, its data are kept stored and those of the new packet are rejected. But, if the sensor node from which the new packet is received has a better RSSI, then the stored ID and RSSI are replaced by the data from this sensor node, and the counter is reset. This process is repeated for each packet received from a parent node candidate. When the counter reaches a limit value, N, the multihop configuration ends by setting the hop to the sensor node of the stored ID. Finally, a new broadcast informs the candidates that they can stop sending packets to the sensor node. In the process of multihop configuration, the period of the packets sent by a candidate to a parent sensor is shorter than that used for the packets sent to the BS in normal operation. In a mobile network where the situation of the nodes is constantly changing, the longer this period is, the more the RSSI received in each packet will differ. In consequence, the

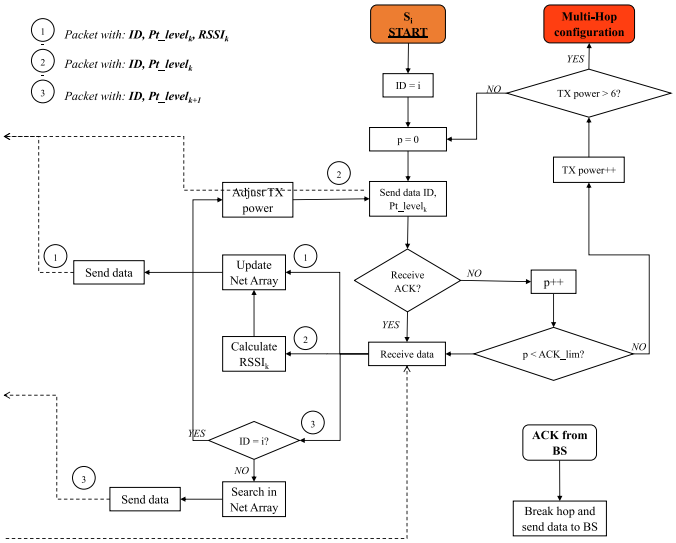

Fig. 12. Updated adjustment phase diagram with the multihop Grey-FTPC transmission and network vector handling.

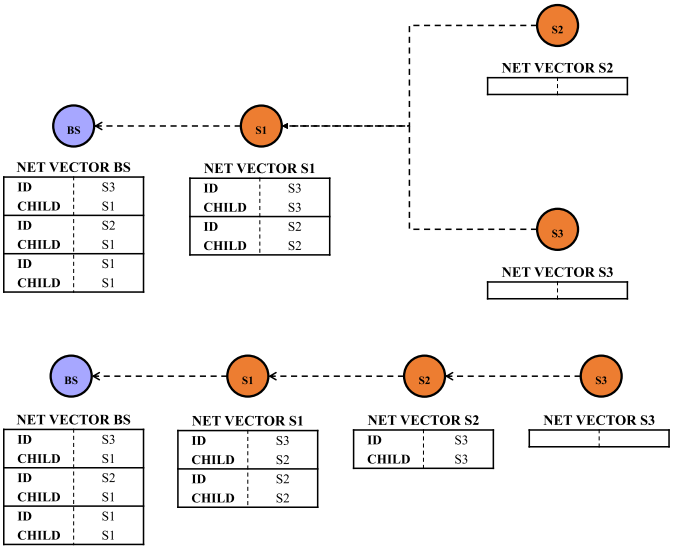

Fig. 13. Creation and update of the network vector at each sensor node for multihop Grey-FTPC.

comparison between candidates will be longer and the counter will take longer to reach the limit value because it will be reset more frequently. Therefore, this parameter can be dynamically adjusted according to the mobility conditions of the target scenario.

3) Implementation of the New Transmission Path: When the node becomes disconnected from the BS, the multihop configuration will choose a new parent node to recover the communication. The parent node receives a packet with the ID and Pt_level_k of the child sensor. In the parent node, the RSSI of the transmission between the parent and the child is calculated and added to the packet as RSSI_k to be analyzed by the algorithm. A network vector is implemented at every node to store the information received from each child sensor. In each element of the vector, the packet ID (which corresponds to the WSN node ID) and the ID of the child sensor from which it has been received are stored. For a packet ID different from those already stored in the vector, a new element of the vector is used. However, if the packet ID is already included in the vector, the corresponding element is updated with the information of the new packet. The network vector allows using the same path with which the packets arrive at the algorithm to send the control packets generated by the algorithm back to the sensor node. When a node receives a control packet it first compares the packet ID with its ID. If they match, it means that the packet was addressed to this node, so it updates the power to the indicated in the packet. But, if they do not match, it has to send the packet to the intended node. Searching for the packet ID in the network vector returns the child sensor to which the packet has to be sent. Although a new parent node has been configured, the node still tries to recover the direct connection to the BS. It is implemented that for every K packets sent using the configured hop (with K being a configurable parameter based on the stability and mobility of the network), the sensor node tries to send the next packet directly to the BS. If the response to this attempt is an *ACK*, then the hop is immediately broken, and the BS is recovered as the parent node. Otherwise, the node will retry after another K packets are sent. The diagram in Fig. 12 shows the AP of the sensor node after the implementation of multihop, handling up to three different types of packets in the communication depending on the information they contain. Fig. 13 represents the network vectors at each of the nodes for the two possible cases of the third case proposed in the multihop approach in Fig. 10.

D. Distinction Between Stable and Unstable Scenarios

The WSN may suffer signal strength interferences, especially when the network performs in indoor scenarios where there are more obstacles, such as walls or doors, including the RSSI from this interference in the GM, results in an unnecessary variation of the transmission power if it exceeds the limits of the fuzzy level where it was located. The experimentally designed fuzzy controller for the use of Cookies as sensor nodes contains RSSI fuzzy levels with a range of 5-dBm each. A disturbance that causes a change in RSSI_{k+1} of 5 dBm, is enough to modify the fuzzy level and cause one of these unnecessary power variations. A possible solution to this problem would be to increase the size of the fuzzy level intervals. The drawback of this approach is that the intervals were initially determined consistently based on experimental results and increasing them would lose the established relationship between the fuzzy levels and the RSSI values. For example, an RSSI considered as H, by increasing the intervals may be considered as HM or even M. This results in a completely different power optimization than the expected one for which the fuzzy levels were originally designed. Furthermore, assuming that the extension of the intervals is done in a way that is centered on the M level, then the extreme levels H and L would be inefficient because they would cover RSSI intervals at the limit of the sensors' operating range.

Therefore, the alternative solution has to be consistent with the initial relationship established for the fuzzy levels, and the range used for the set of levels. The implemented improvement meets both conditions by removing the intermediate levels HM

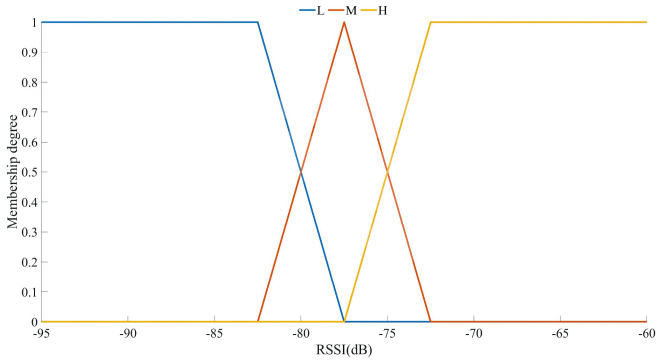

Fig. 14. Definition of the fuzzification of the real RSSI range for unstable/indoor environments.

TABLE IV
RSSI FUZZY LEVEL INTERVALS ACCORDING TO THE EXPERIMENTAL RANGES FOR INDOOR ENVIRONMENTS

RSSI fuzzy	RSSI crisp
L	[-inf, -85]
M	[-85, -75]
H	[-75, inf]

TABLE V
OPTIMIZATION OF THE NUMBER OF FUZZY INFERENCE RULES FOR THE TRANSMISSION POWER CONFIGURATION IN INDOOR ENVIRONMENTS

Rule	$RSSI_k$	$RSSI_{k+1}$	inc
1	H	H	-1
2	H	M	-1
3	H	L	0
4	M	H	-1
5	M	M	0
6	M	L	1
7	L	H	0
8	L	M	1
9	L	L	1

and LM. The HM level is now considered as H level while the LM level will be considered as M. Thus, the same range of dBm is divided between only three levels: 1) H; 2) M; and 3) L. The intervals will be larger allowing to decrease the effect of disturbances. Table IV shows these intervals and Fig. 14 shows the triangular functions of the fuzzy levels.

The fuzzy rules are modified to those in Table V. The power increase does not exceed one step in absolute value. Therefore, the disadvantage of this improvement is a slower response to abrupt changes.

This controller based on three fuzzy levels will be used for sensor network deployments in indoor scenarios where there are more disturbances, while in outdoor scenarios the controller based on five fuzzy levels will be used.

E. Readjustment of the Transmission Power Set by the Prediction Model

The fuzzy controller is designed according to experimental results obtained from real network deployments. However, the transmission power set by the algorithm is not always optimal. When a sensor node has a low RSSI then it increases its power until the RSSI reaches a stable value, entering the LM level. Contrarily, a sensor node with a high RSSI decreases its power until the RSSI M level is reached. The lowest power consumption in the node is achieved for the lowest possible RSSI within the stable range, i.e., at the LM level. In conclusion, the fuzzy controller used obtains the optimal power consumption if the transmission power of a sensor node is configured by increasing it. A new phase (NP) is implemented in the algorithm, and it can be initiated on demand from the BS. In this phase, an SP is executed again once normal network operation has started. The SP configures the minimum transmission power of each sensor node, with the possibility that decreasing the power decreases the received RSSI. In this case, the algorithm will bring the RSSI value up to the LM level by increasing the power, thus obtaining an improvement in terms of the optimal power consumption once the node is in a stable state.

TABLE VI
NETWORK PARAMETERS AND TEST CHARACTERISTICS FOR THE PERFORMANCE EVALUATION

Parameter	Values
Hardware node	CC2520-based Cookies
Communication layer	IEEE 802.15.4
Network size	5, 20, 60
Network topology	Single-hop, Multi-hop
Environment	Indoor, Outdoor
Speed of movement (max)	5 m/s
Transmission period	2 sec.

V. PERFORMANCE EVALUATION AND ANALYSIS OF THE GREY-FTPC IN THE IOT COOKIES PLATFORM

In this section the performance evaluation and analysis of the Grey-FTPC implementation, including the proposed adaptations within the IoT Cookies platform is detailed. First, a set of functional verification tests have been carried out to see how the system implementation behave under several network conditions. Then, a power consumption analysis and comparison of the solution with other transmission power strategies is discussed.

A. Functional Tests of the Grey-FTPC

The performance of the implemented Grey-FTPC and the specific contributions have been tested through a real WSN. For this purpose, the initial parameters to setup the evaluation tests are summarized in Table VI. The Cookie setup used for the deployment of the sensor nodes includes the ADuC841-based processing, CC2520-based communication and power supply layers that compose the modular sensor nodes. The communication stack used to test the real system is based on the IEEE 802.15.4, which is one of the most widely used standard for low-power resource-constrained WSN and IoT, although the proposed system implementation can be extrapolated to other communication stacks. The node identified with an $ID = 1$ is assigned to the BS, leaving the rest of the sensor nodes according to the notation used as S2, S3, S4, S5, and so on. These nodes receive power from a battery to enable them to move in the operating space. The energy supplied by the batteries is managed by the appropriate power

setting determined by the Grey-FTPC. The BS is in a static position connected to a PC through a USB interface, and the Grey engine is implemented in C. Thus, the PC is the power source of the BS. By performing the test procedure up to 5 times using different node locations, an equivalent network grid of 20 sensor nodes is achieved. The speed of movement of the nodes does not exceed 5 m/s and the packet transmission period is 2 s.

In the design of the network maps used in the tests, theoretical relationship between the distance from the sensor node to the BS and the received signal has not been considered. In an ideal situation, the RSSI is the same at all points on a circumference with the BS as the center. However, this situation does not apply in reality due to interference, especially in indoor scenarios. Therefore, the points where the sensor nodes will be placed in the tests are decided experimentally. A previous study determines areas where the sensor nodes use different levels of transmission power configured as minimum power. This way, it is verified that the Grey-FTPC performs correctly when the configured power is similar to the one obtained in this study. Although the exact distance of these zones from the BS is not measured, it is confirmed that the further the zone is from the BS, the higher transmission power is used.

The system has been repeatedly tested several times for periods of hours during different performance journeys, and here a subset of representative moving transitions and transmission power window changes are represented to show how the system behaves in such variable conditions. With these measurement sets the following states are represented: consecutive sensor node mobility for dynamic single and multihop system assessment; RSSI stable/uniform versus RSSI fluctuation conditions for TX power reconfiguration response; transitions between minimum and maximum configuration levels for TPC adaptability evaluation; and tied (within central configuration values) versus wide TX power windows. The results are plotted based on the values of PT_level_k and RSSI_k obtained at a time instant against the values of PT_level_{k+1} and RSSI_{k+1} predicted by the Grey-FTPC for the same time.

1) Testing Grey-FTPC Without Multihop Strategy in WSN: Initially, the performance of the Grey-FTPC and the other contributions implemented, except for the multihop strategy, is tested using all available sensor nodes. Fig. 15 shows a characteristic RSSI peak when the sensor node starts to move closer to the BS. The transmission power of the node is adjusted to minimum levels as it approaches the BS. When the node stops, the power continues changing until the RSSI is within the fuzzy M or LM levels according to the fuzzy rules. Therefore, the transmission power of a node must be constant if it is not moving. However, because the RSSI suffers interference even when the sensor node is stationary, a power fluctuation may appear between two consecutive levels as observed from 80 s onward in the graph.

Fig. 16 corresponds to the performance of another sensor node for the same indoor test. Again, the transmission power changes only with characteristic RSSI peaks. Fig. 17 shows the same test for this node but outdoors. Due to the use of five fuzzy levels the RSSI intervals with reduced intervals, the peaks required for power variation are smaller. The consequence is more frequent changes in the transmission power.

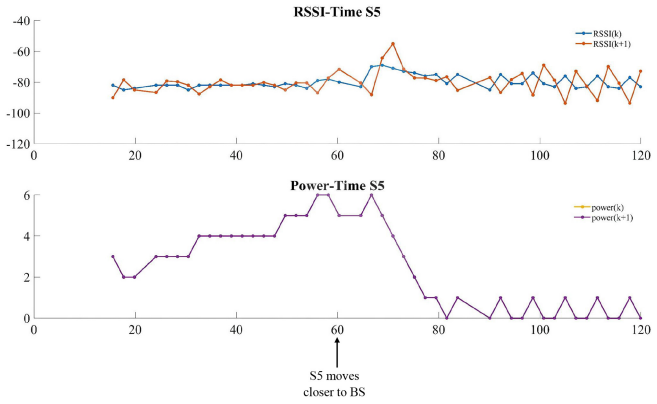

Fig. 15. Comparison of the measured RSSI, predicted RSSI, and configured transmission power for S5 in the first test case.

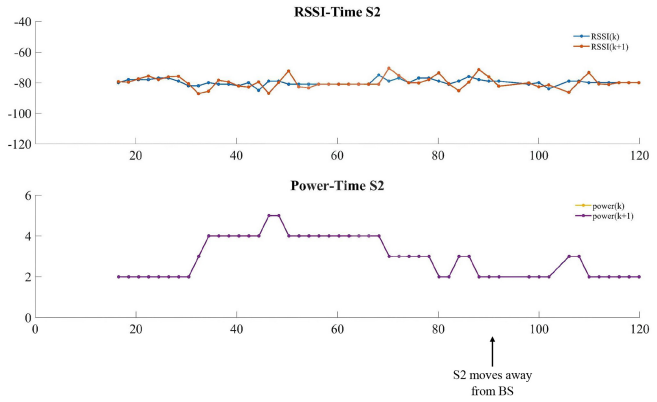

Fig. 16. Comparison of the measured RSSI, predicted RSSI, and configured transmission power for S2 in the first test case.

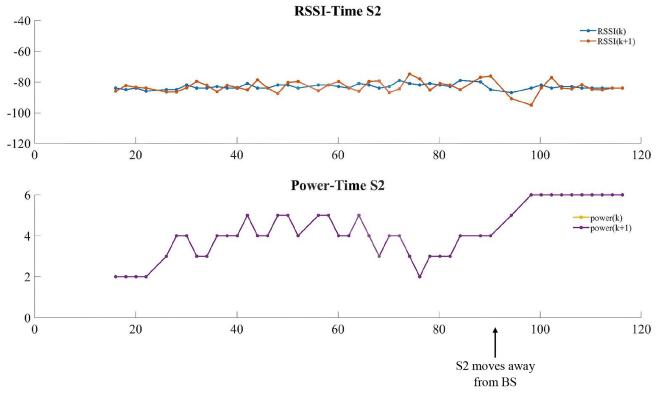

Fig. 17. Comparison of the measured RSSI, predicted RSSI, and configured transmission power for S2 in the first test case (outdoor).

2) Testing Grey-FTPC With Multihop Strategy in WSN: In a second test, the performance of the multihop implementation is first demonstrated in a network with two sensor nodes, S2 and S3, besides the BS. Node S2, which was located close to the BS, moves away by rapidly losing communication. The transmission power starts to increase automatically attempting to recover the connection with the BS. Once the maximum

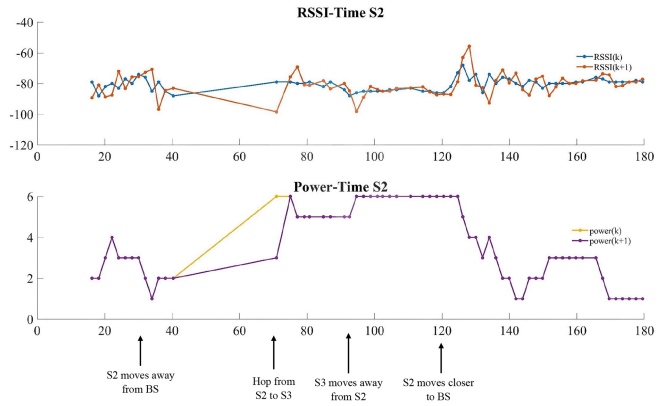

Fig. 18. Comparison of the measured RSSI, predicted RSSI, and configured transmission power for S2 in the second test case (multihop) where the sensor nodes perform several movements.

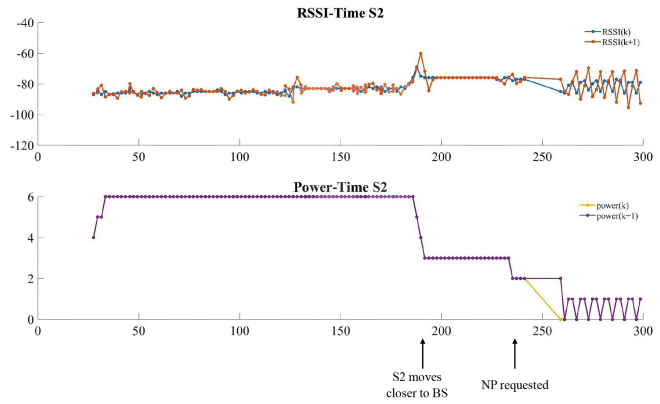

Fig. 19. Comparison of the measured RSSI, predicted RSSI, and configured transmission power for S2 in the third test case (multihop) with higher mobility and NP process during the test.

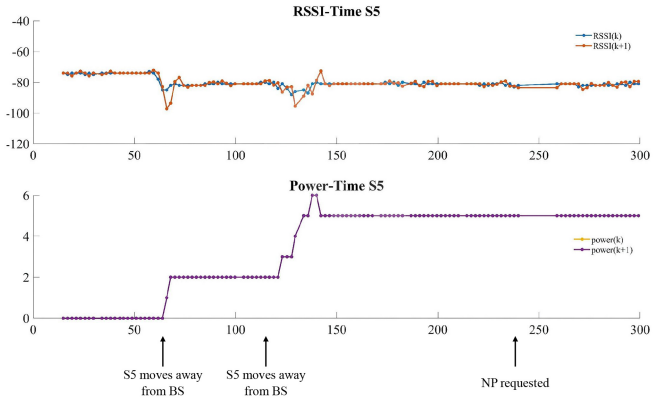

Fig. 20. Comparison of the measured RSSI, predicted RSSI, and configured transmission power for S5 in the third test case (multihop) with higher mobility and NP process during the test.

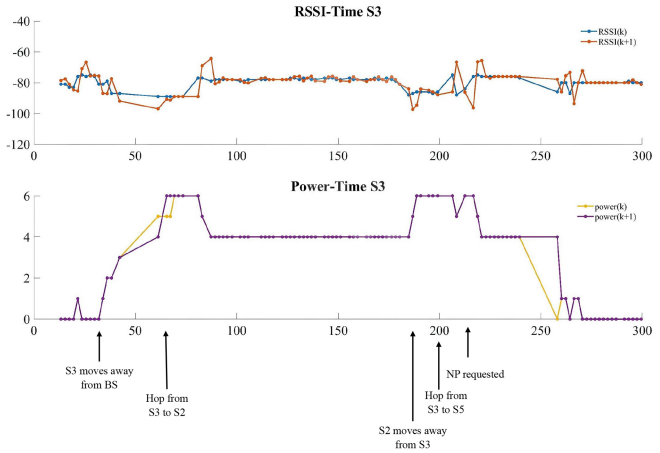

Fig. 21. Comparison of the measured RSSI, predicted RSSI, and configured transmission power for the third test case showing the different moving phases from the S3 perspective.

power level is reached, as the packets sent by S2 are still not received, it starts the multihop configuration. The chosen parent sensor is the only available candidate, S3. After the configuration is completed, the communication with the BS is recovered with the new transmission path. The algorithm adjusts the transmission power for the new link from S2 to S3. When the distance between the two sensor nodes increases, a negative RSSI peak appears, and consequently the power increases. Finally, S2 moves to a point near the BS. The hop to S3 is broken giving preference to the direct connection with the BS. The algorithm then adjusts the transmission power for this link, decreasing the power as S2 moves closer to the BS. Fig. 18 shows the performance of S2 for this second test case.

The last test case allows the performance verification of all the implementations developed in a network with the four available sensor nodes and the BS. At each step of this process, a different sensor node is moved. In addition, the time between the execution of one step and the next is 30 s. Thus, the algorithm has time to adjust the transmission power for the new stationary situation of the node after it changes its position.

Figs. 19 and 20 correspond to the indoor test for sensor nodes S2 and S5, respectively. Both nodes move to areas within the range of the BS, so multihop is not needed. When they start their movement, characteristic RSSI peaks appear and lead to an adjustment to new transmission power. Power level stability is again observed when the sensor node is static. At 240 s, an NP is requested to set the minimum power for all nodes in the network. In the case of S2, the transmission power decreases compared to the power set by the algorithm. However, for S5 the power after the NP matches the power previously set by the algorithm.

The sensor node S3 in Fig. 21 moves closer to node S2 while moving away from the BS and losing communication with it. The power is automatically increased until it reaches the maximum level which is not enough to recover the connection with the BS. Therefore, the multihop configuration is executed choosing S2 as the parent sensor with the best RSSI among all the candidate nodes. Once the connection with the BS is recovered with the new transmission path established, a high-RSSI peak is observed. The algorithm responds to this peak for the new link between S2 and S3 by decreasing the transmission power. After 180 s, the parent sensor S2 starts to move away from S3. The algorithm increases the power to the maximum level but ends up losing communication again. Therefore, another multihop configuration is executed

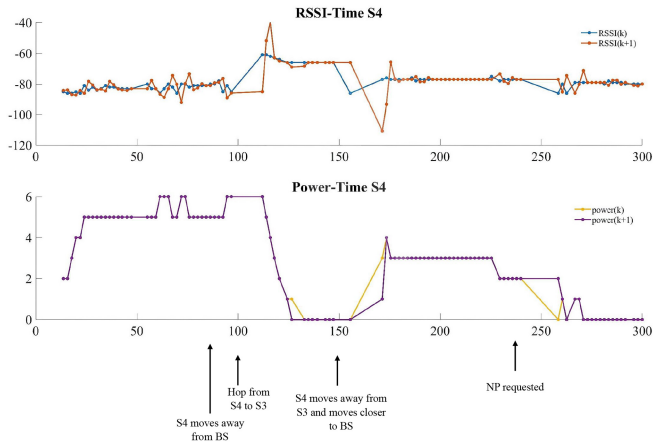

Fig. 22. Comparison of the measured RSSI, predicted RSSI, and configured transmission power for the third test case showing the different moving phases from the S4 perspective.

TABLE VII
CHARACTERISTICS CONSIDERED FOR THE POWER CONSUMPTION ANALYSIS

Parameter	Values
Power consumption (TX)	48.6 mW (level 0) 59.7 mW (level 1) 69.3 mW (level 2) 74.7 mW (level 3) 77.4 mW (level 4) 86.1 mW (level 5) 93.1 mW (level 6)
Power consumption (RX)	55.5 mW
Weight per packet bit	32 us
$RSSI_{min}$	-85 dBm
S	20
D	10
N	3
TX power adaptation	Single-hop, Multi-hop
Sensor data packet size	80 bytes
Grey-FTPC control bytes	5 bytes

choosing S5 as the new parent sensor, which had been moved closer to S3 previously. Finally, this hop is broken when the direct connection of the sensor node S3 to the BS is re-established when it moves closer to the BS.

The sensor node S4 initially also moves away from the BS and loses communication with it, requiring a hop to another node. According to the network node distribution during the multihop configuration, S4 can choose either S2 or S3 as the parent sensor. The movement of S4 ends in a position next to S3. Therefore, if S3 is chosen as the parent sensor as in Fig. 22, when the algorithm starts adjusting the power for this new link a significant RSSI spike appears. Consequently, the transmission power will drop from the maximum level before the multihop to the minimum level. At the end of the test, S4 moves closer to BS. Due to the abrupt change, communication with the parent sensor is lost and the transmission power starts to increase automatically. When S4 re-establishes a direct connection with the BS the hop is broken.

B. Power Consumption Analysis

Based on the aforementioned tests and in order to study the impact of the proposed system on the node/network power consumption, a comparative analysis of the Grey-FTPC has been carried out. Apart from the considered scenarios and states, additional parameters are taken into account for this power consumption evaluation, such as the percentage of reconfiguration, according to the dynamic conditions, so that the network overhead when applying Grey-FTPC can be seen. Moreover, the solution is compared to MaxPow and W-TPC, which are two alternatives for transmission power configuration. The first one considers the maximum configuration level during the network lifetime, so no additional control overhead is needed (fixed transmission power value). The second one carries out a series of measurements to establish a TX Power level W for a minimum RSSI band RSSI_{min}, which is used in normal operation unless data loss is experimented (through ACK monitoring). In case data is lost after N consecutive retries, the MaxPow strategy is used until an RSSI value is kept above an S threshold, during D consecutive cycles. Table VII summarizes the main node and network characteristics considered for the power consumption comparison analysis, apart from those already set for the performance assessment.

Apart from the evaluation and measurement setup composed of the Cookie processing and power supply layers that allow power profiling the sensor nodes and can provide an additional debugging interface to verify the measurement data from the Cookie platform when needed, the power consumption has also been characterized with the help of USB power consumption meters connected to the Cookie node. The modularity of the Cookie hardware architecture [27] allows analyzing different layer stack setups, which is useful for distinguishing and separating different power shifts of the connected hardware.

From the real measurements and packet transmission monitoring of the network, energy is computed considering the consumption of the communication layer of the Cookie hardware node, contrasted with the values from the IEEE 802.15.4 transceiver, for every transmission power configuration, and taking the other cookie layer consumption as common offset for the energy comparison, to evaluate the energy consumption increment relatively between the various transmission power cases, and thus to define the impact of the proposed control strategies in the sensor node/network. Then, the weight per packet bit, which is the time unit to transmit the packet (common to the different strategies) is considered together with the packet lengths, which depends on the transmission control strategy.

For the power consumption analysis the Grey-FTPC overhead is included, considering that the periodic sensor data transmission (upstream) is used to send control data from the sensor nodes to de BS, so no additional control messages are sent in those cases. When a TX power reconfiguration is needed, a control message has to be sent (downstream) to the corresponding sensor node. the packet overhead size is 5 bytes. In case no reconfiguration of TX power is needed, control packets will not be emitted, thus no additional power

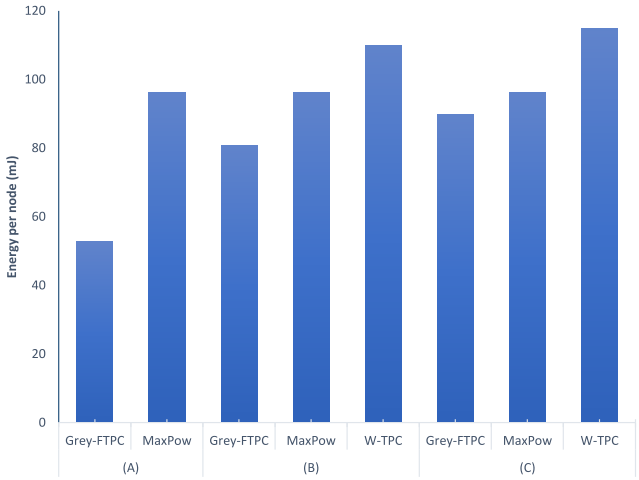

Fig. 23. Comparison of the TPC strategies for each group of network conditions (single hop).

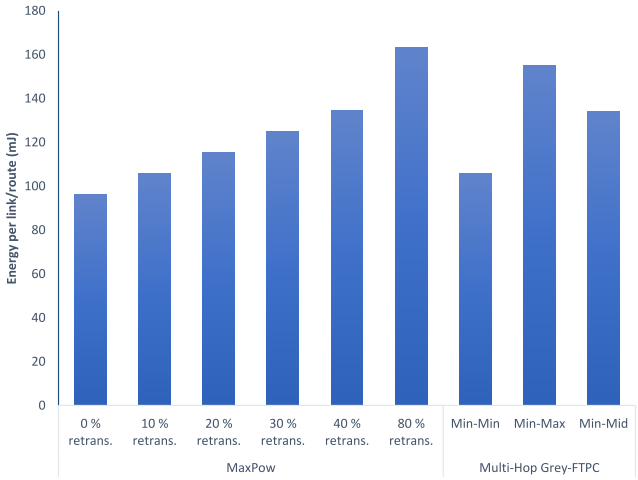

Fig. 24. Energy consumption comparison of the TPC strategies for border hop conditions.

consumption overhead in such situation. The power consumption comparison is first performed for single-hop scenarios and then for multihop scenarios. For the former one, three different states are compared as follows.

1) Stable environment (A), with limited variability and movements, where Grey-FTPC can select low-configuration levels with minimum reconfiguration actions.
2) Dynamic environment (B), where Grey-FTPC works in intermediate levels (as in Fig. 16) with a percentage of reconfiguration packets with respect to data packets (20% in this case).
3) High-dynamic environment (C), where the number of reconfiguration packets with respect to data packets is high (as in Fig. 17), which corresponds to high movements and/or unstable signal conditions (43% in this case).

Fig. 23 shows the results of the average energy consumption per node for a transmission window of 100 packets in each solution. It can be seen that the Grey-FTPC outperforms the other solutions in all the scenarios, with a peak of 45% of energy gain with respect to MaxPow for (A). As expected, the differences reduce as the number of reconfigurations and thus the control overhead increases, yet with a gain of almost 7% in case of having high instability and mobility (close to 50% of reconfigurations needed). The differences are higher compared to W-FTPC (10%), which corresponds to a worst behavior of that solution in situations where higher peaks of RSSI fluctuations and sensor node mobility appears, in contraposition to Grey-FTPC which allows keeping the quality values stable, while keeping the less power-hungry transmission power level. When there are not very high and frequent fluctuations in configurations, the energy gains are enhanced, such as in case of (B) with 20% of overhead. In that particular case, the Grey-FTPC obtained a 26% of energy reduction with respect to W-FTPC.

On the other hand, the multihop scenario is compared with MaxPow (which shows better results than W-TPC) in border conditions, that is, in those situations where the MaxPow configuration is in the limit of minimum connectivity (close to $RSSI_{min}$), which may affect the quality of data delivery as the number of retransmissions increases. In such situations, the multihop Grey-FTPC would benefit both the power consumption and the delivery service (beyond such border conditions multihop Grey-FTPC will indeed outperforms MaxPow and single-hop Grey-FTPC, because the later ones will not provide a valid transmission power configuration that assure coverage with the BS). In order to compare the impact of both solutions in these conditions, the following percentage of retransmissions range for MaxPow is computed: [0, 20, 30, 40, 80]. While in the first value the border state does not impact in the number of retransmissions, in the last one almost every message needs to be resent. For multihop Grey-FTPC, the control overhead and the power consumption of both links that allow reconfiguring the connection with the parent node are taken into account. For this, the following scenarios are considered to compute the average energy consumption per route: 1) minimum level in both hops; 2) minimum and maximum levels in both hops, respectively; and 3) minimum and medium levels in both hops, respectively.

Fig. 24 shows the energy consumption results per link (MaxPow) and route (multihop Grey-FTPC). It can be seen that in case of MaxPow (0), it is slightly below the rest of multihop Grey-FTPC values, and actually the Grey-FTPC (no multihop) shall obtain similar results as there is no need of establishing a new route due to the cero rate of retransmissions. When the percentage of retransmissions increase to 20%, the multihop Grey-FTPC starts having better results for the Min-Min scenario, while for the 80% of retransmissions, the energy gain is above 35%. Moreover, for 40% even the Min-Mid obtain better results than MaxPow, with 21% of gain for Min-Min. For the case of Min-Max, this scenario is beneficial in case of having 70%–80% of retransmissions.

Finally, the multihop scenario results are extended considering a network composed of 60 nodes. If the degree of multihop routes with respect to border links can be extrapolated as a subset of sensor nodes in the network, a comparison between MaxPow and multihop Grey-FTPC is

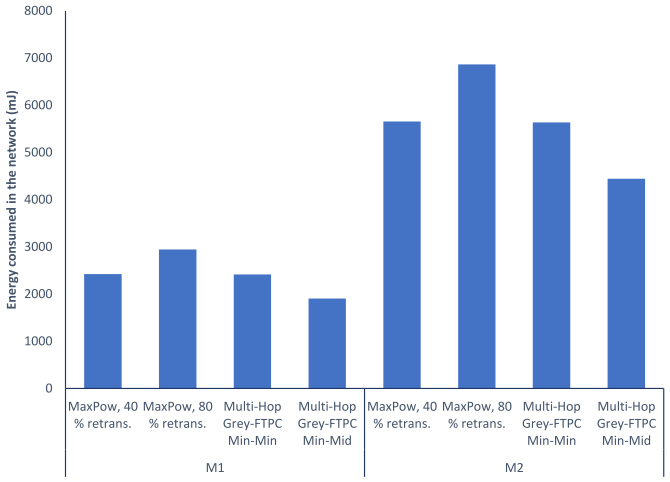

Fig. 25. Energy consumption comparison of MaxPow and multihop Grey-FTPC cases for 60 node-based network conditions.

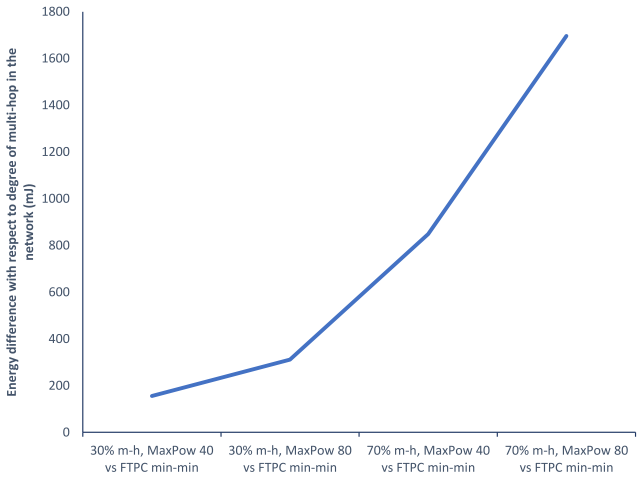

Fig. 26. Energy consumption difference between MaxPow and multihop Grey-FTPC cases in relation with the degree of multihop routes.

shown in Fig. 25 considering 30% (M1) and 70% (M2) values. For the MaxPow the transmission percentage range is [20, 40], while for the multihop Grey-FTPC the Min-Min and Min-Mid cases are used. As expected, when the number of sensor nodes scale the worst the number of retransmissions the benefits of multihop Grey-FTPC will be higher. To better see this relationship, Fig. 26 represents the difference between the worst case scenario (MaxPow with 80% of retransmissions) and multihop Grey-FTPC with a Min-Min scenario, multiply by the degree of multihop routes, showing that the slop of the curve increases rapidly as the number of sensor nodes is higher in the network.

C. Discussion

The experimental test cases allowed verifying the proposed multihop Grey-FTPC implementation on the IoT Cookie sensor platform, including all the optimization capabilities proposed for the improved solution. It has been checked that when the sensor node is stationary, the received RSSI_k is more constant, around -80 dBm, and similar to RSSI_{k+1}. These values are within the LM and M fuzzy levels where the transmission power does not change as stated in the fuzzy rules. The RSSI peaks that cause a power adjustment have been obtained when the sensor node starts to move and when it hops to another node. The more the signal strength of a new link in a hop differs from the previous link signal strength, the more significant the RSSI peak will be. For the same peak size, the transmit power suffers more variations in outdoor scenarios.

The automatic adjustment of the transmit power by the node and the multihop configuration ensure the communication of the sensor nodes within the range of the BS and even extend this communication to areas outside its range. As confirmed by the experimental results, the algorithm does not distinguish in the input data the type of link it is analyzing, whether it is a direct connection from the sensor to the BS or a hop, so the multihop network improvement provides a seamless adaptation to the network topology without the need to modify the structure of the Grey fuzzy-inference-based prediction engine. Moreover, it has been verified that the NP request improves the power adjustment of the algorithm at a given time during network operation.

Regarding the energy consumption outcomes, it has been verified that the implementation of Grey-FTPC could lead to obtain benefits with respect to other alternatives even with the overhead needed for the control strategy. Depending on the instability of the network, the degree of reconfigurations, and the number of retransmission conditions, the benefits of the solution in terms of energy gain can go from 14% to almost 40% (case of the 60 node network). Furthermore, apart from the fact that other strategies do not consider the coverage limitation and the multihop configuration as in case of the proposed optimization, for border cases where coverage is within the minimum values for data transmission the multihop Grey-FTPC exhibits better results than MaxPow, depending on the percentage of retransmissions and thus the quality of the communication between sensor and parent node.

VI. Conclusion and Future Work

The Grey-FTPC implemented in a real WSN platform for the Extreme Edge of IoT efficiently adjusts the transmission power to the movement of the sensor nodes for optimal battery consumption. The predictive model has been built only with the last four RSSI data received. For the design of the fuzzy controller, the intervals of each RSSI fuzzy level have been experimentally selected according to the network properties. If the intervals are narrow, the controller will be faster to changes in the signal, but it can also become more sensitive to disturbances. The implementation of two operating modes with different numbers of fuzzy levels gives the flexibility to adapt the algorithm depending on the stability of the network to interference. The in-node embedded implementation of the multihop Grey-FTPC support for more diverse network deployments and sensor distributions allows extending the performance of the optimization engine to more realistic IoT sensor networks, without modifying the prediction dynamics, as it is implemented such that the optimization engine carried out the transmission power reconfiguration in a seamless

manner. Results exhibit important gains both in terms of functionality and energy consumption reduction, as the proposed solution achieves above 40% of gains in comparison with MaxPow and W-TPC solutions. As shown in the experimental tests, although the percentage of benefits will depend on several network conditions, the proposed system will provide better results in the majority of scenarios compared to the other configurations. Directions for future work include autonomous and dynamic identification of network stability and consequent automatic adaptation of the fuzzy controller based on the proposed optimization. Moreover, the deployment of a greater amount of nodes is envisioned to test the performance of the overall system in denser sensing scenarios, including the integration of the main grey engine in an embedded edge device, such as a single board computer.

REFERENCES

[1] B. Chander, S. Pal, D. De, and R. Buyya, "Artificial intelligence-based Internet of Things for industry 5.0," *Artif. Intell. Based Internet Things Syst.*. Cham, Switzerland: Springer, pp. 3–45, 2022.

[2] G. Mujica, J. Henche, and J. Portilla, "Internet of Things in the railway domain: Edge sensing system based on solid-state LIDAR and fuzzy clustering for virtual coupling," *IEEE Access*, vol. 9, pp. 68093–68107, 2021.

[3] B. Pradhan, S. Bhattacharyya, and K. Pal, "IoT-based applications in healthcare devices," *J. Healthc. Eng.*, vol. 2021, pp. 1–18, Mar. 2021.

[4] F. J. Dian, R. Vahidnia, and A. Rahmati, "Wearables and the Internet of Things (IoT), applications, opportunities, and challenges: A survey," *IEEE Access*, vol. 8, pp. 69200–69211, 2020.

[5] D. Davcev, K. Mitreski, S. Trajkovic, V. Nikolovski, and N. Koteli, "IoT agriculture system based on LoRaWAN," in *Proc. 14th IEEE Int. Workshop Factory Commun. Syst. (WFCS)*, 2018, pp. 1–4.

[6] Y. Wu, "Cloud-edge orchestration for the Internet of Things: Architecture and AI-powered data processing," *IEEE Internet Things J.*, vol. 8, no. 16, pp. 12792–12805, Aug. 2021.

[7] M. De Donno, K. Tange, and N. Dragoni, "Foundations and evolution of modern computing paradigms: Cloud, IoT, edge, and fog," *IEEE Access*, vol. 7, pp. 150936–150948, 2019.

[8] K. Xu, Y. Qu, and K. Yang, "A tutorial on the Internet of Things: From a heterogeneous network integration perspective," *IEEE Netw.*, vol. 30, no. 2, pp. 102–108, 2016.

[9] Y. Teng, M. Liu, F. R. Yu, V. C. Leung, M. Song, and Y. Zhang, "Resource allocation for ultra-dense networks: A survey, some research issues and challenges," *IEEE Commun. Surveys Tuts.*, vol. 21, no. 3, pp. 2134–2168, 3rd Quart., 2018.

[10] M. H. Miraz, M. Ali, P. S. Excell, and R. Picking, "Internet of Nano-Things, things and everything: Future growth trends," *Future Internet*, vol. 10, no. 8, p. 68, 2018.

[11] J. Portilla, G. Mujica, J.-S. Lee, and T. Riesgo, "The extreme edge at the bottom of the Internet of Things: A review," *IEEE Sensors J.*, vol. 19, no. 9, pp. 3179–3190, May 2019.

[12] J. M. Williams et al., "Weaving the wireless Web: Toward a low-power, dense wireless sensor network for the Industrial IoT," *IEEE Microw. Mag.*, vol. 18, no. 7, pp. 40–63, Nov./Dec. 2017.

[13] M. Capra, R. Peloso, G. Masera, M. Ruo Roch, and M. Martina, "Edge computing: A survey on the hardware requirements in the Internet of Things world," *Future Internet*, vol. 11, no. 4, p. 100, 2019.

[14] S. Lin et al., "ATPC: Adaptive transmission power control for wireless sensor networks," *ACM Trans. Sensor Netw. (TOSN)*, vol. 12, no. 1, pp. 1–31, 2016.

[15] J.-S. Lee and Y.-C. Lee, "An application of grey prediction to transmission power control in mobile sensor networks," *IEEE Internet Things J.*, vol. 5, no. 3, pp. 2154–2162, Jun. 2018.

[16] P. Pace, G. Fortino, Y. Zhang, and A. Liotta, "Intelligence at the edge of complex networks: The case of cognitive transmission power control," *IEEE Wireless Commun.*, vol. 26, no. 3, pp. 97–103, Jun. 2019.

[17] L. Wang, G. Zhang, J. Li, and G. Lin, "Joint optimization of power control and time slot allocation for wireless body area networks via deep reinforcement learning," *Wireless Netw.*, vol. 26, pp. 4507–4516, May 2020.

[18] A. H. Sodhro, S. Pirbhulal, G. H. Sodhro, A. Gurtov, M. Muzammal, and Z. Luo, "A joint transmission power control and duty-cycle approach for smart healthcare system," *IEEE Sensors J.*, vol. 19, no. 19, pp. 8479–8486, Oct. 2019.

[19] W. Lee, N. Kim, and B.-D. Lee, "An adaptive transmission power control algorithm for wearable healthcare systems based on variations in the body conditions," *J. Inf. Process. Syst.*, vol. 15, no. 3, pp. 593–603, 2019.

[20] X. Chen, M. Ma, and A. Liu, "Dynamic power management and adaptive packet size selection for IoT in e-healthcare," *Comput. Electr. Eng.*, vol. 65, pp. 357–375, Jan. 2018.

[21] J. L. Hill and D. E. Culler, "Mica: A wireless platform for deeply embedded networks," *IEEE micro*, vol. 22, no. 6, pp. 12–24, Nov./Dec. 2002.

[22] Q. Zhou, K. Zheng, L. Hou, J. Xing, and R. Xu, "Design and implementation of open LoRa for IoT," *IEEE Access*, vol. 7, pp. 100649–100657, 2019.

[23] M. S. Philip and P. Singh, "Adaptive transmit power control algorithm for dynamic LoRa nodes in water quality monitoring system," *Sustain. Comput., Inform. Syst.*, vol. 32, Dec. 2021, Art. no. 100613.

[24] R. W. Coutinho, A. Boukerche, and A. A. Loureiro, "A novel opportunistic power controlled routing protocol for Internet of Underwater Things," *Comput. Commun.*, vol. 150, pp. 72–82, Jan. 2020.

[25] I. A. Hayder et al., "Towards controlled transmission: A novel power-based sparsity-aware and energy-efficient clustering for underwater sensor networks in marine transport safety," *Electronics*, vol. 10, no. 7, p. 854, 2021.

[26] P. Merino, G. Mujica, J. Señor, and J. Portilla, "A modular IoT hardware platform for distributed and secured extreme edge computing," *Electronics*, vol. 9, no. 3, p. 538, 2020.

[27] G. Mujica, V. Rosello, J. Portilla, and T. Riesgo, "Hardware-software integration platform for a WSN testbed based on cookies nodes," in *Proc. 38th Annu. Conf. IEEE Ind. Electron. Soc.*, 2012, pp. 6013–6018.

[28] "CC2520 IEEE 802.15.4 RF transceiver for the 2.4 GHz ISM band," Data sheet CC2520, Texas Instrum., Dallas, TX, USA, 2007.

[29] "ADuC841 20MIPS 8052 flash MCU," Data sheet ADuC841, Analog Devices, Inc., Wilmington, MA, USA. Accessed: Apr. 10, 2023.

Guillermo Moreno received the B.Sc. degree in industrial technologies engineering from the Universidad Politécnica de Madrid, Madrid, Spain, in 2021, where he is currently pursuing the M.Sc. degree in industrial engineering.

His research interests focus on applying novel technologies to improve the wireless communication and dynamic multihop topologies of wireless sensor networks in real application context, as well as implementing embedded algorithms to optimize the performance and power consumption of sensor nodes.

Gabriel Mujica (Member, IEEE) received the Ph.D. degree in industrial electronics engineering from the Universidad Politécnica de Madrid (UPM), Madrid, Spain, in 2017, with the International Distinction and Outstanding Doctorate Award.

He is an Associate Professor and a Research Member with the Center of Industrial Electronics, UPM, where he is mainly involved in the areas of Internet of Things, networked embedded systems and wireless sensor networks (WSN). He has participated in different national and European research projects (including Horizon 2020 Projects), related to the development and optimization of WSN, as well as the integration of heterogeneous IoT edge hardware, software, and communication technologies for wireless distributed systems, with a particular focus on the performance evaluation and optimization of sensor platforms under real deployment contexts. He has authored several contributions in high-impact conferences and journals. He has collaborated in the organization of research tutorials and seminars, and as a reviewer and a Guest Editor in international conferences and indexed journals. Moreover, his visiting research stay with Trinity College Dublin, Dublin, Ireland, strengthened the vision and applicability of IoT technologies for smart and sustainable cities, leveraging collaborations in the area of distributed systems within such contexts. His current main research interests are related to multihop distributed networks for the extreme edge of IoT, and hardware–software co-design and communication protocols for IoT embedded systems in smart urban and industrial application scenarios.

Jorge Portilla (Senior Member, IEEE) received the M.Sc. degree in physics from the Universidad Complutense de Madrid, Madrid, Spain, in 2003, and the Ph.D. degree in electronic engineering from the Universidad Politécnica de Madrid (UPM), Madrid, Spain, in 2010.

He was a Visiting Researcher with the Industrial Technology Research Institute, Hsinchu, Taiwan, in 2008, and also with the National Taipei University of Technology (Taipei Tech), Taipei, Taiwan, in 2018, working on wireless sensor networks hardware platforms and network clustering techniques. He is currently an Associate Professor with the UPM. He carries out his research activity within the Centro de Electrónica Industrial, UPM. He has participated in more than 30 funded research projects, including European Union FP7 and H2020 Projects, and Spain Government Funded Projects, as well as private industry funded projects, mainly related to wireless sensor networks and Internet of Things. He has numerous publications in prestigious international conferences as well as in journals with impact factor. His research interests are focused on wireless sensor networks, Internet of Things, digital embedded systems, and reconfigurable FPGA-based embedded systems.

Jin-Shyan Lee (Senior Member, IEEE) received the Ph.D. degree in electrical and control engineering from National Chiao Tung University, Taipei, Taiwan, in 2004.

From 2005 to 2009, he was a Researcher with the Information and Communications Research Laboratory, Industrial Technology Research Institute (ITRI), Hsinchu, Taiwan. He then joined the Department of Electrical Engineering, National Taipei University of Technology, Taipei, where he is currently a Professor. Since then, he is also an Adjunct Researcher with the ITRI. From 2003 to 2004 and from 2015 to 2016, he was a Visiting Scholar with the Department of Electrical and Computer Engineering, New Jersey Institute of Technology, Newark, NJ, USA. His current research interests include Internet of Things, wireless sensor networks, Petri nets, and intelligent systems.